Supporting Information

A bioinspired monolayer gel with efficient omnidirectional moisture-driven actuation for humidity sensing

Sampurna Routray,[a] Malay Kumar Baroi,[a] Ritvika Kushwaha,[a] Priyam Das,[a] Debapratim Das[a]*

[a] Department of Chemistry, Indian Institute of Technology Guwahati, Assam 781039, India

Experimental Section

Materials

Branched polyethylenimine (BPEI; M_n ~ 10,000 by GPC) was purchased from Sigma-Aldrich. Polyethylene Glycol Diacrylate (PEGDA; n = approx. 9) (stabilized with MEHQ) was purchased from TCI. Acrylamide (AAm) and Ammonium persulphate (APS) were procured from SRL. Dodecyl acrylate (DDA), Tetradecyl acrylate (TDA), Hexadecyl acrylate (HDA), Octadecyl acrylate (ODA), and 2-hydroxy-N,N,N-trimethylethanaminium chloride (commercial name: Choline Chloride) were purchased from BLD Pharmatech (India) Private Limited. Ethyl alcohol (HPLC grade) was procured from TEDIA. All of the materials were used without further purification. Silicone moulds with a size of 3.4 cm × 3.4 cm × 3.2 cm, a Digital Wall Clock Hygrometer Thermometer with Humidity Meter, and a Mini LCD Digital thermometer sensor were commercially purchased.

Fabrication of monolayered moisture-responsive BP@ODA actuator

The actuator was fabricated utilising a casting-evaporation strategy. It consisted of the following steps. Firstly, homogeneous solutions of BPEI, PEGDA, ODA, AAm, and APS in ethanol were prepared. The BPEI solution (10wt%) along with PEGDA solution (30wt%) was cast in a silicone mould, followed by the addition of a solution of AAm (1wt%) and APS (0.1wt%). The mixed solution was then left undisturbed for an hour for subsequent solvent evaporation at room temperature (25 °C). Then, a solution of ODA (1 wt% in ethanol) was coated on top of it and further allowed to dry for an hour at room temperature (25°C). After complete drying, the actuator with one side coated hydrophobically was obtained. Actuators with different hydrophobic coatings, including DDA, TDA, and HDA, were prepared in a similar manner.

Characterization

Morphologies of the gels were characterised using field-emission scanning electron microscopy (FESEM) images obtained on a Gemini SEM 300 (Zeiss) instrument. Energy Dispersive X-ray (EDS) were also performed using a Gemini SEM 300 (Zeiss) instrument. The gels were freeze-dried and adhered to the double-sided carbon tape for FESEM and EDS analysis. The cross-section of the organogel was analysed utilising an EVOS™ XL Core Imaging System (Thermo Fisher Scientific). Water contact angle images were captured using a KRÜSS Drop Shape Analyser DSA-25 with an automatic dispenser at ambient conditions. The chemical structure elucidation before and after the hydrophobic coating was done using a PerkinElmer instrument under ambient conditions. Mechanical properties of the various proportions of the gel samples were measured by a Universal Testing Machine (Instron 5994, USA) on a 100N load cell at 25 °C and 40% RH. P-XRD analysis of the gel samples was carried out using a Rigaku Smartlab wide-angle diffractometer at 9kV. The

diffraction angle ranged from 10° to 80°. Rheological studies of the various gel samples were obtained using an Anton Paar MCR 102 rheometer equipped with a 20 mm parallel plate (with 0.5 mm zero gap) measuring system at 25 °C. The different relative humidity-based experiments were performed in a humidity-controlled chamber with a consistent supply of moisture.

Analysis of the humidity-responsive behaviours of the actuator

The humidity-controlled chamber was designed to analyse the bending performance of the actuator at different percentages of relative humidity (Figure S9). The digital wall clock hygrometer thermometer with humidity meter was placed inside the chamber to monitor the change in the relative humidity throughout the experiment. The relative humidity inside the chamber was regulated by a controlled supply of water vapour. Water was heated at a specific temperature, 50°C, and the resulting vapour was directed into the chamber through a pipe. As time progressed, the concentration of water vapour inside the chamber gradually increased. The BP@ODA actuator was suspended inside the chamber with the help of tweezers. Further, with the gradual increase of humidity inside the chamber, the bending motion of the actuator was captured using a camera positioned at the same level as the actuator. Thereafter, from the snaps and video taken, the bending angle at a particular percentage of humidity was analysed. For the experiments related to the rate of humidity change, water was heated at four different values of temperature. To supply the water vapour at a slower rate, the temperature of the water was maintained at a lower value. Consequently, for a higher rate of humidity change, the water temperature was kept at a higher value.

Supporting Figures

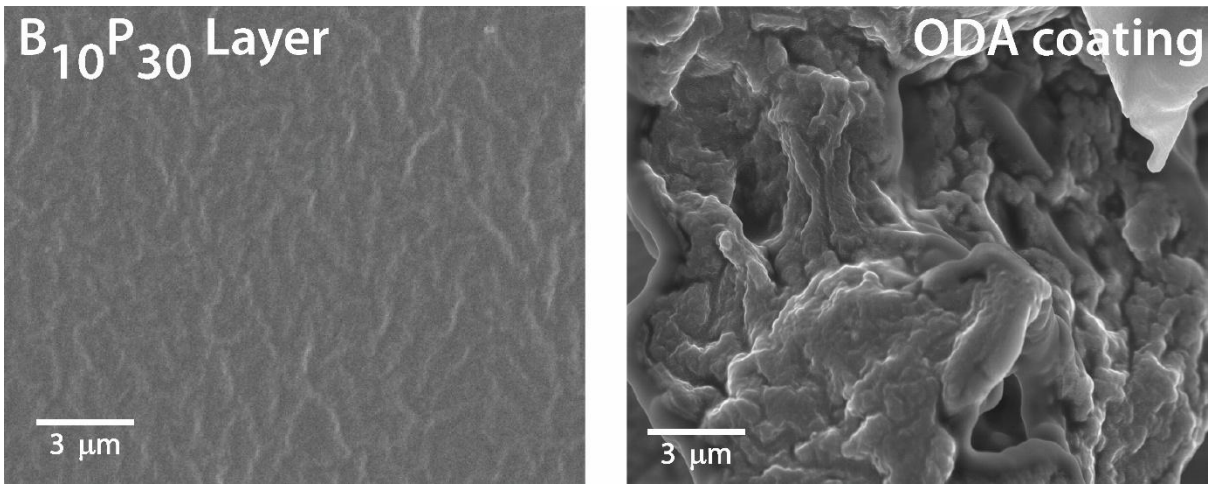

Figure S1. FESEM images of the hydrophilic and hydrophobic surfaces of the actuator.

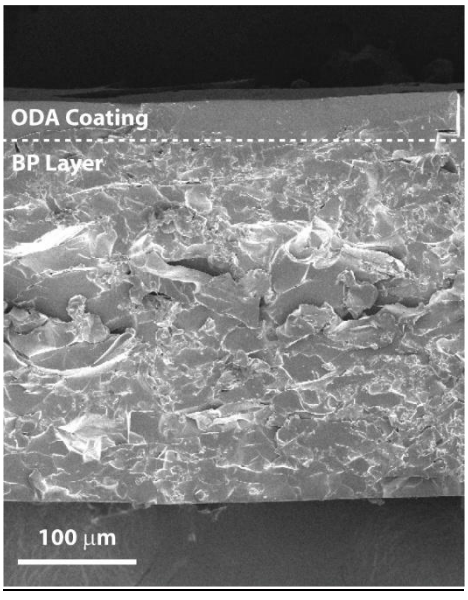

Figure S2. Cross-sectional FESEM image of the BP@ODA gel.

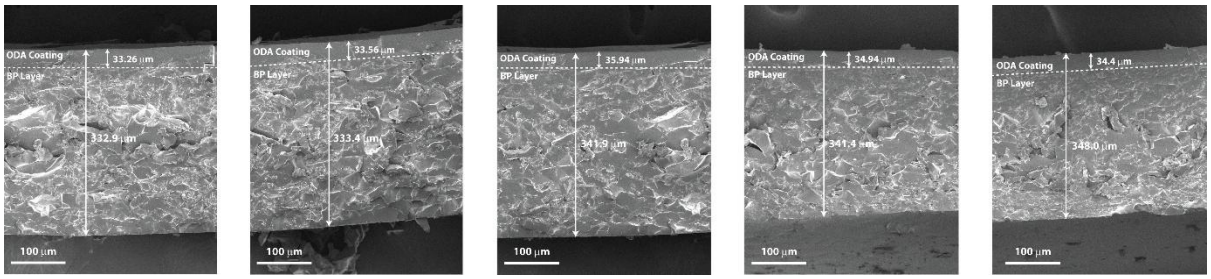

Figure S3. Cross-sectional FESEM images of five different BP@ODA gels prepared independently through identical procedures, demonstrating ODA coating and BP layer of almost equal thickness.

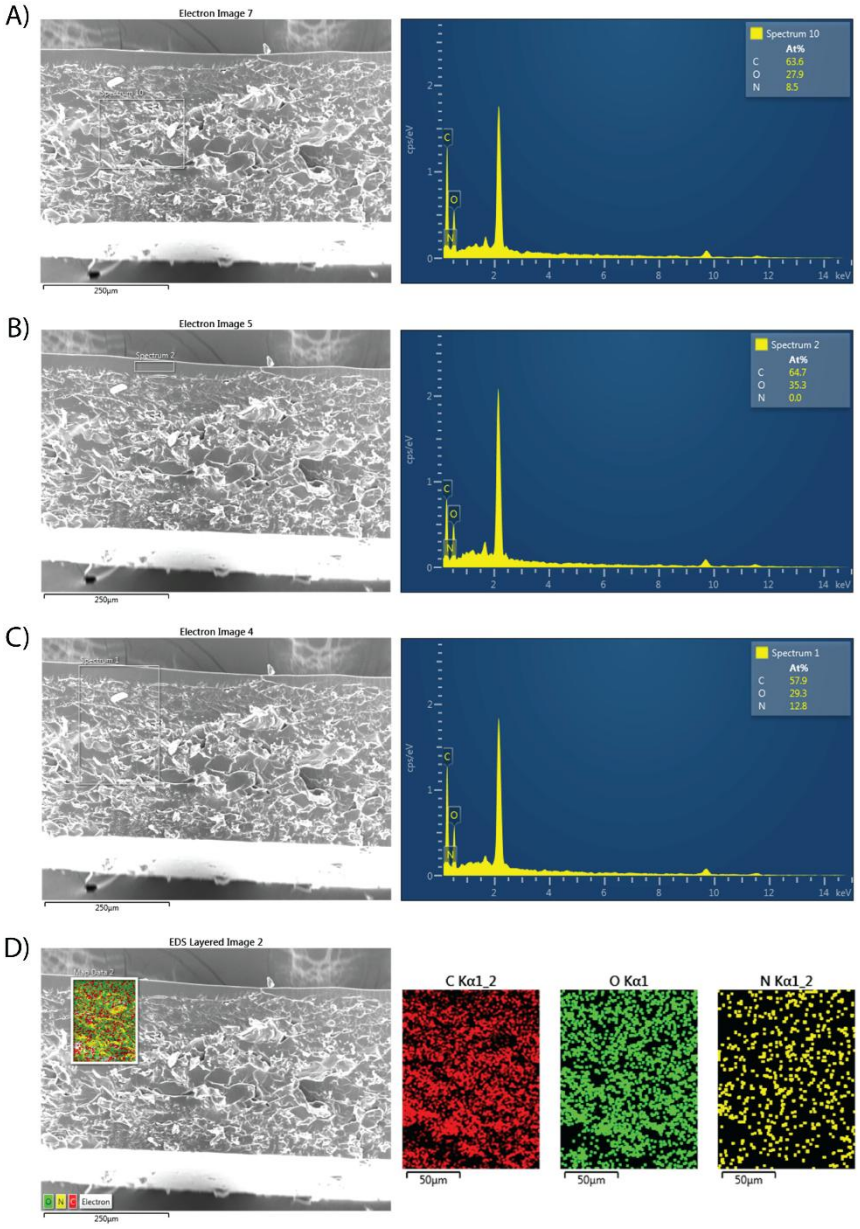

Figure S4. FESEM image of the BP@ODA gel and the corresponding EDS of: A) BP@ODA; B) ODA coating; and C) Elemental mapping of BP@ODA gel.

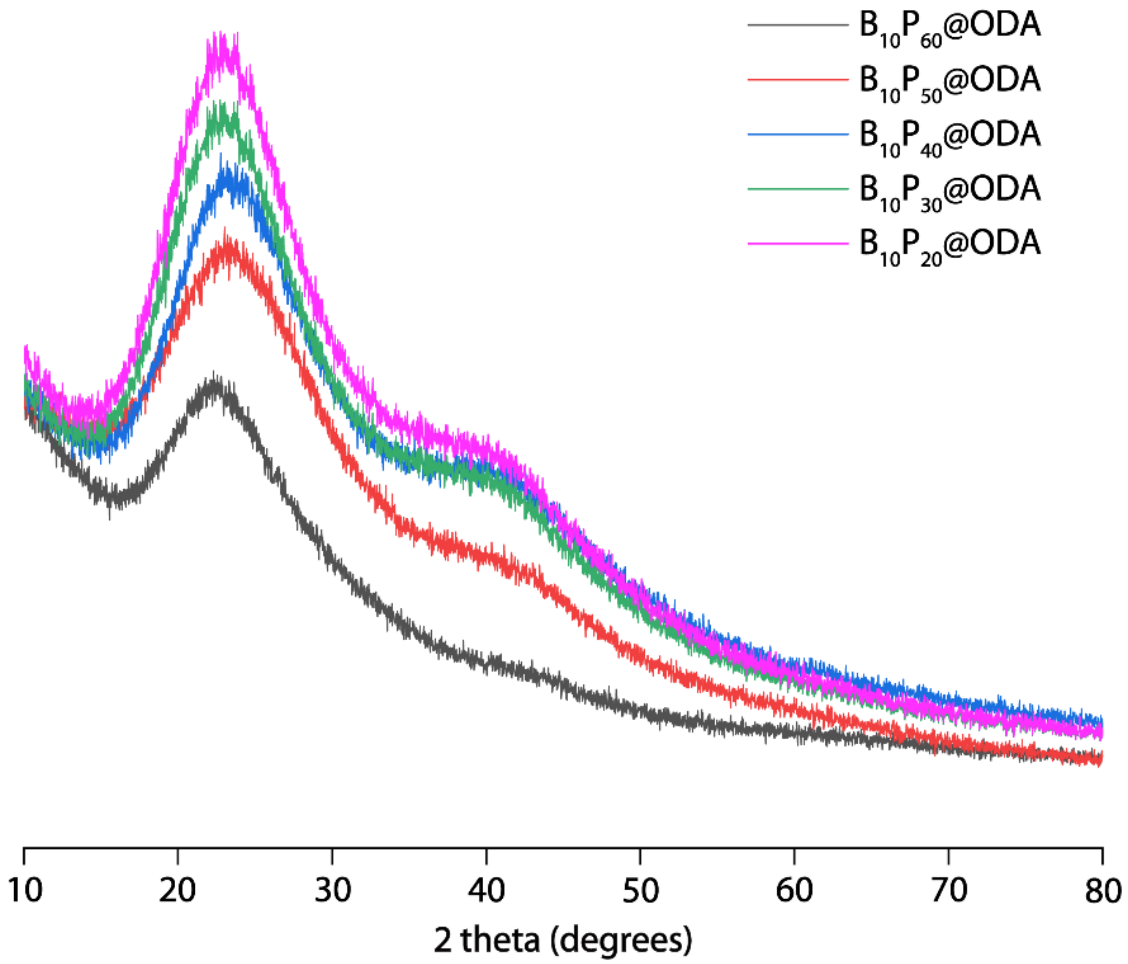

Figure S5. P-XRD analysis of the $B_{10}P_X$@ODA actuator, where "x" varies from 20 wt% to 60 wt%.

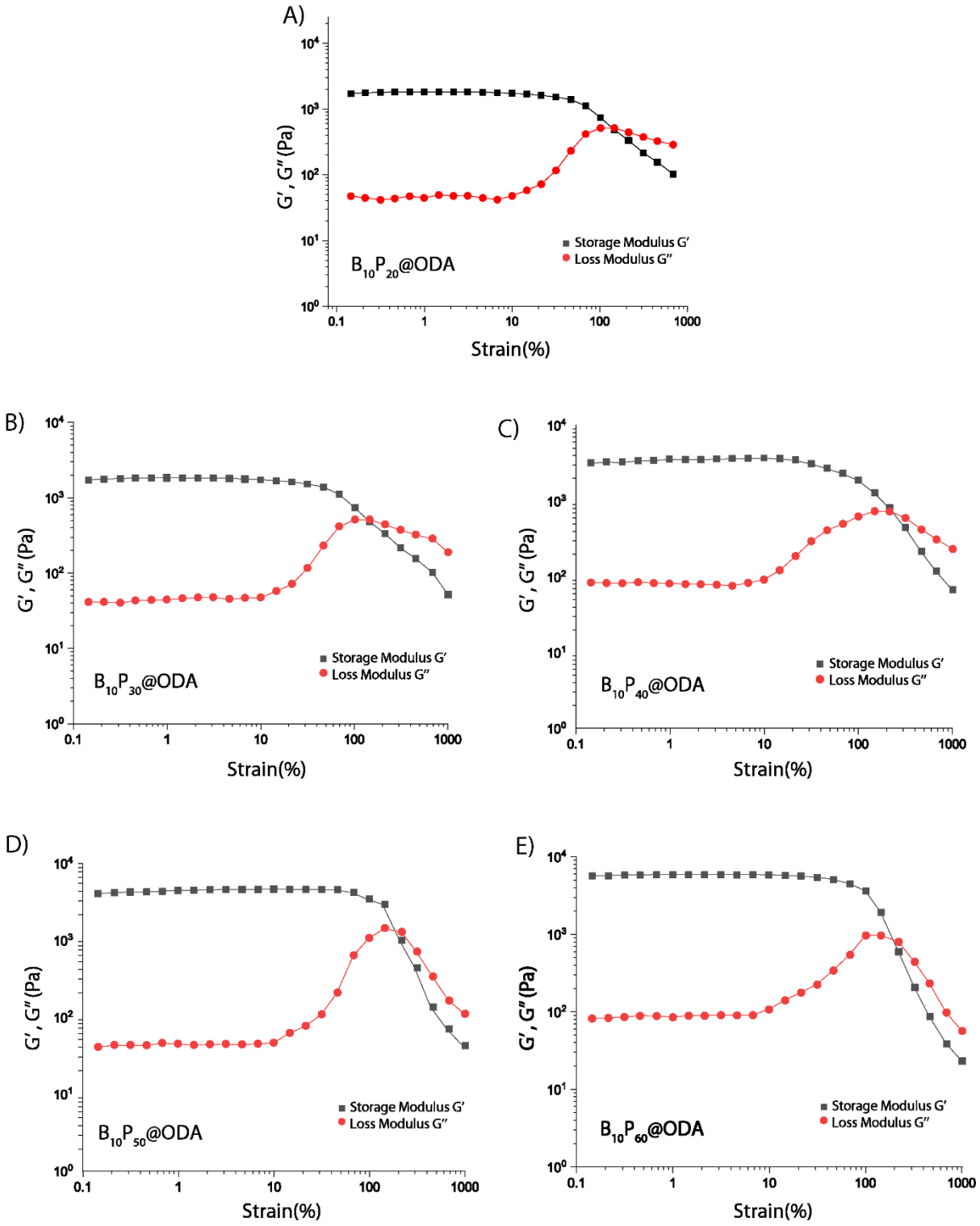

Figure S6. Rheological analysis of the $B_{10}P_X$@ODA actuator where "x" is (a) 20 wt% (b) 30 wt% (c) 40 wt% (d) 50 wt% (e) 60 wt%.

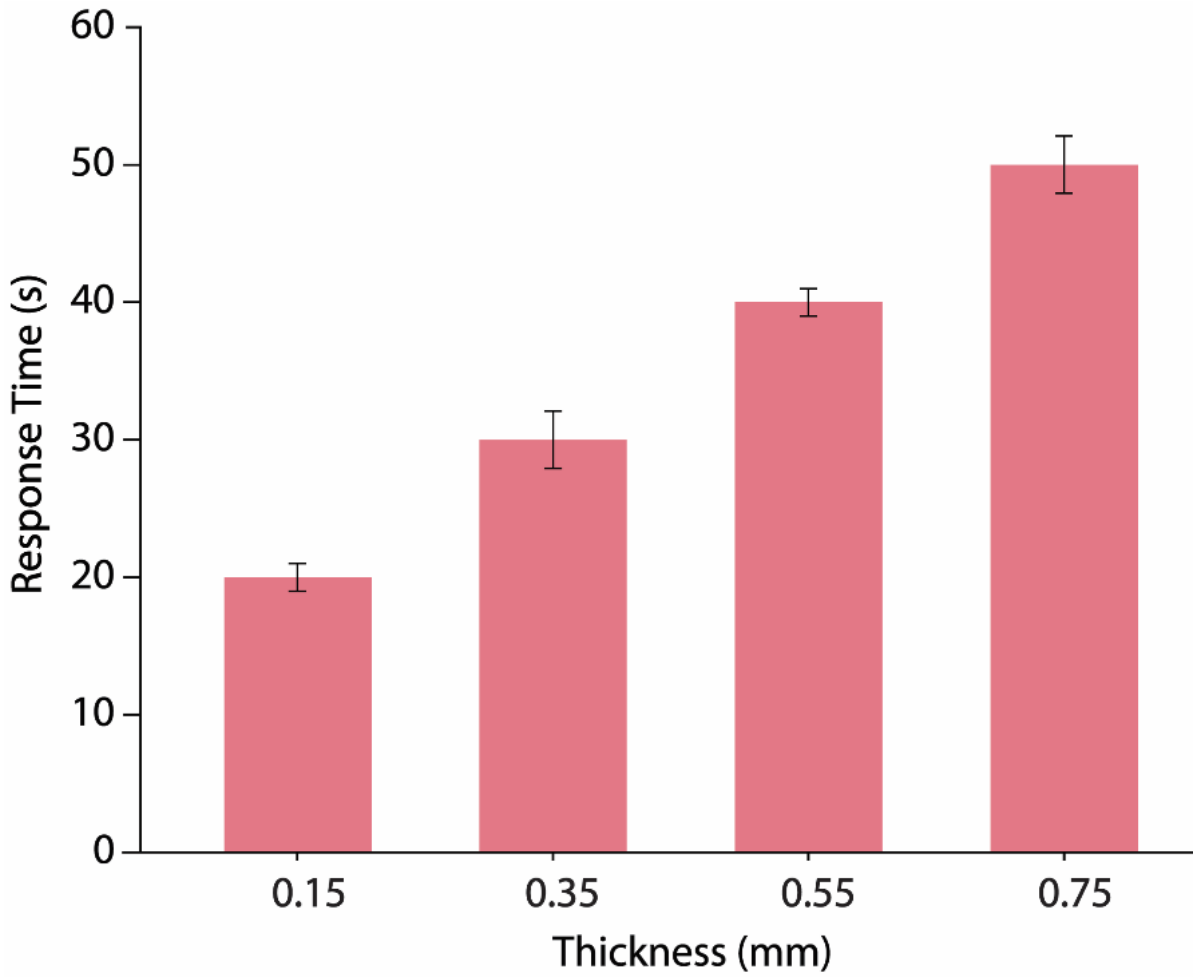

Figure S7. Effect of thickness of BP@ODA gel on the actuation.

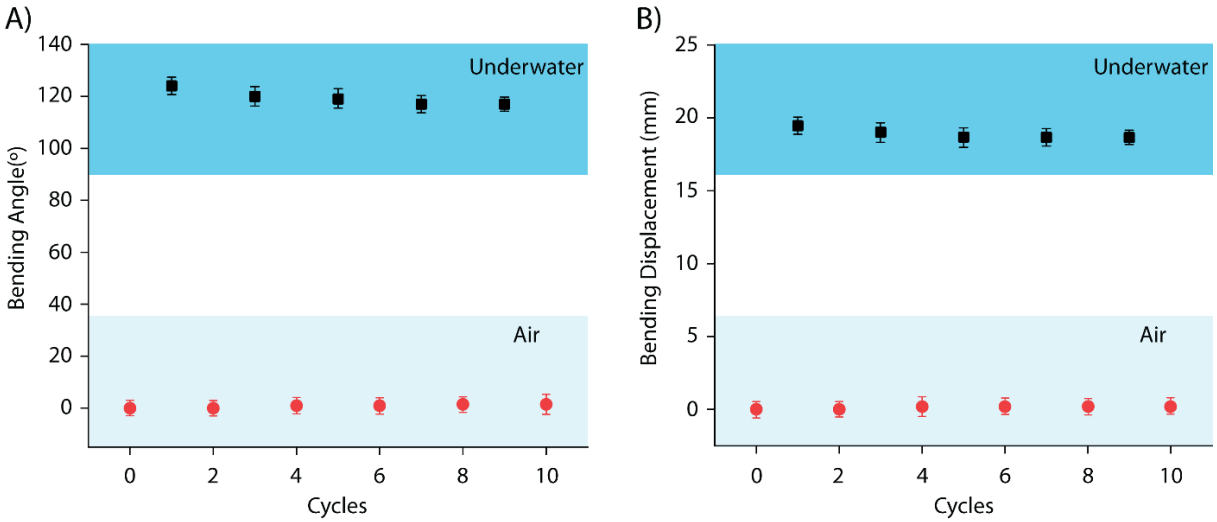

Figure S8. Repeatability of the actuator in terms of: A) Bending Angle; B) Bending Displacement.

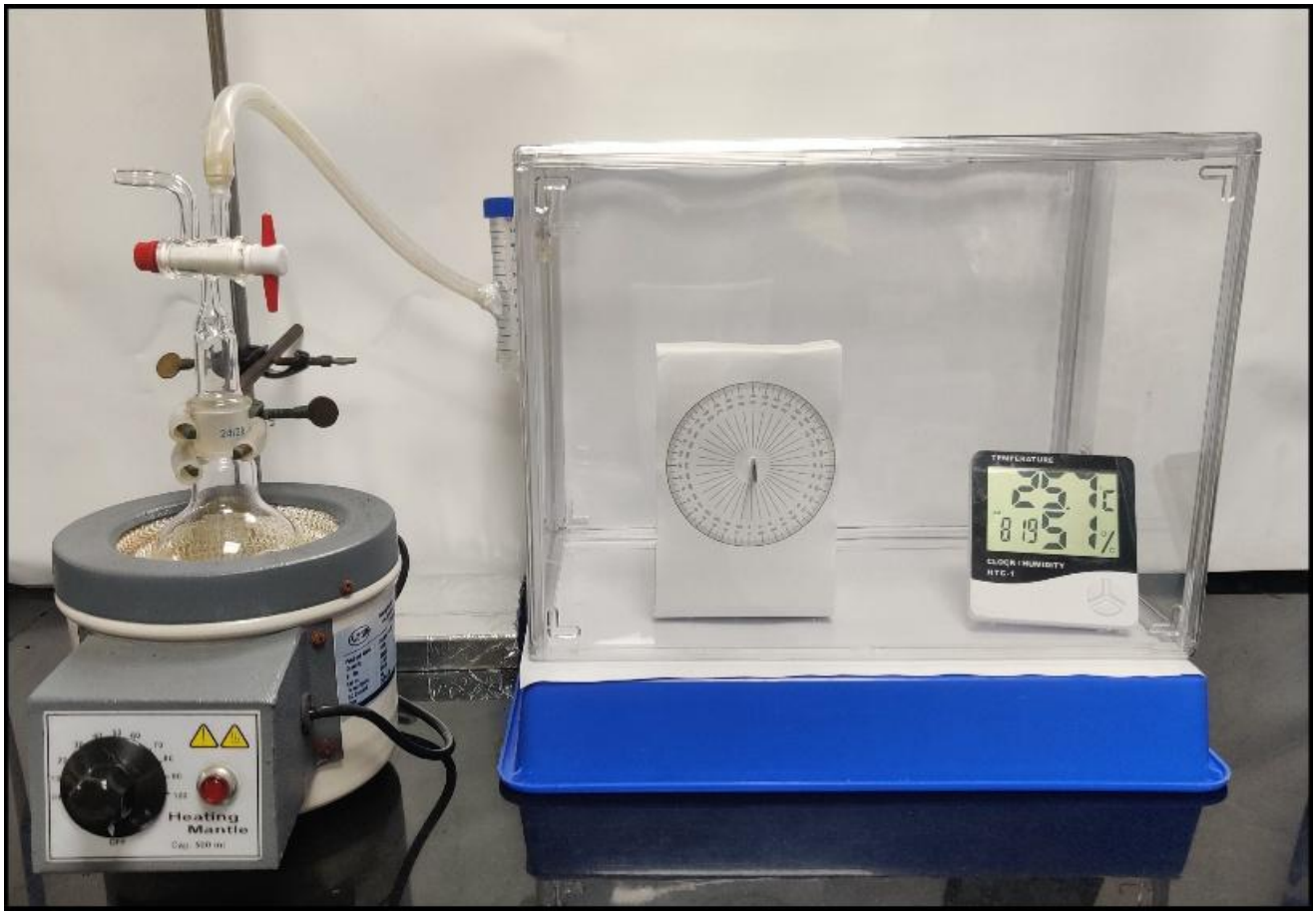

-

Figure S9. Humidity-controlled chamber.

Figure S10. Actuation of $B_{10}P_{30}$@ODA at different humidity levels.

Figure S11. $B_{10}P_{30}$@ODA actuator demonstrating actuation in natural humid conditions.

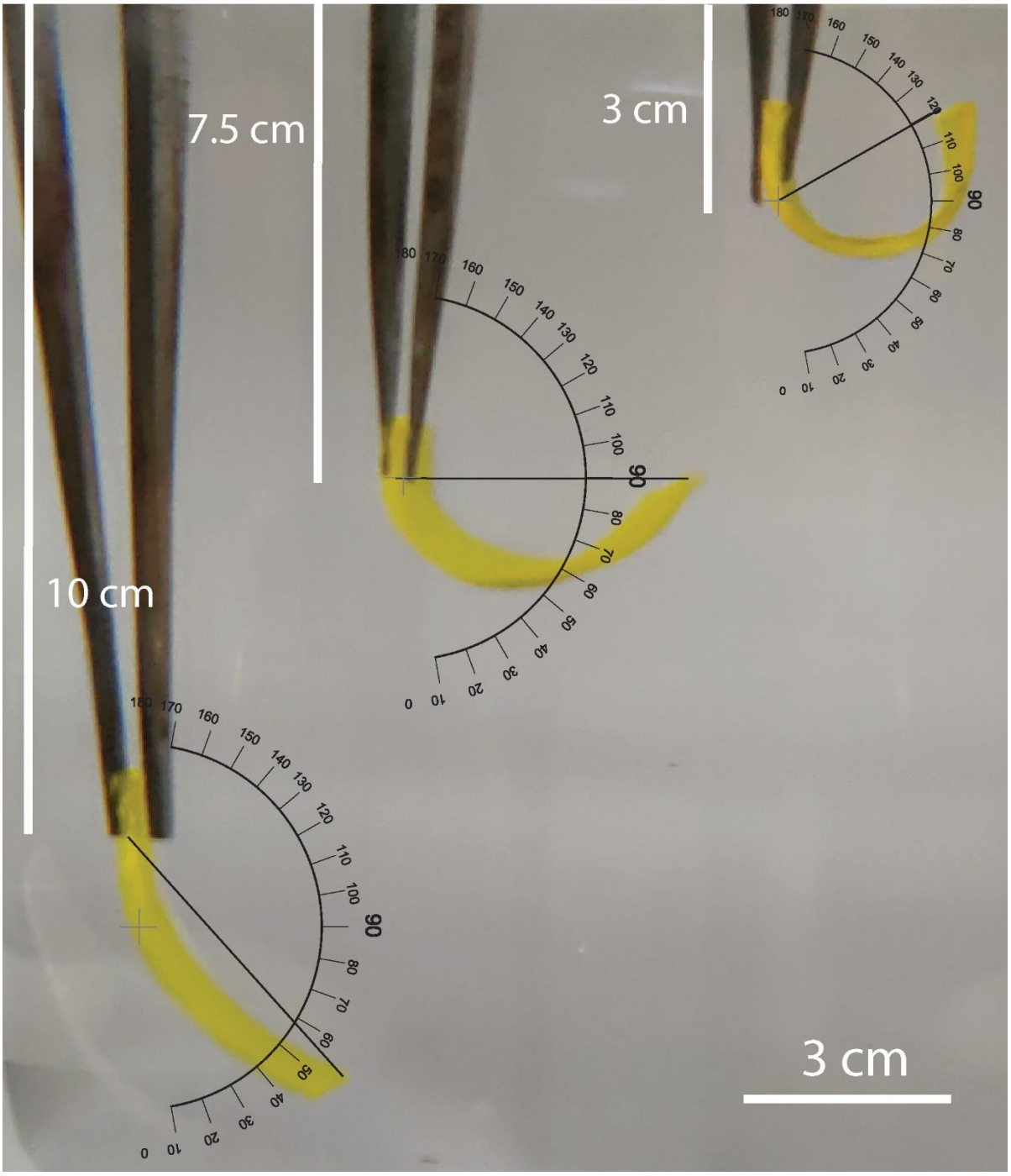

Figure S12. Actuation of $B_{10}P_{30}$@ODA in bulk water at different depths.

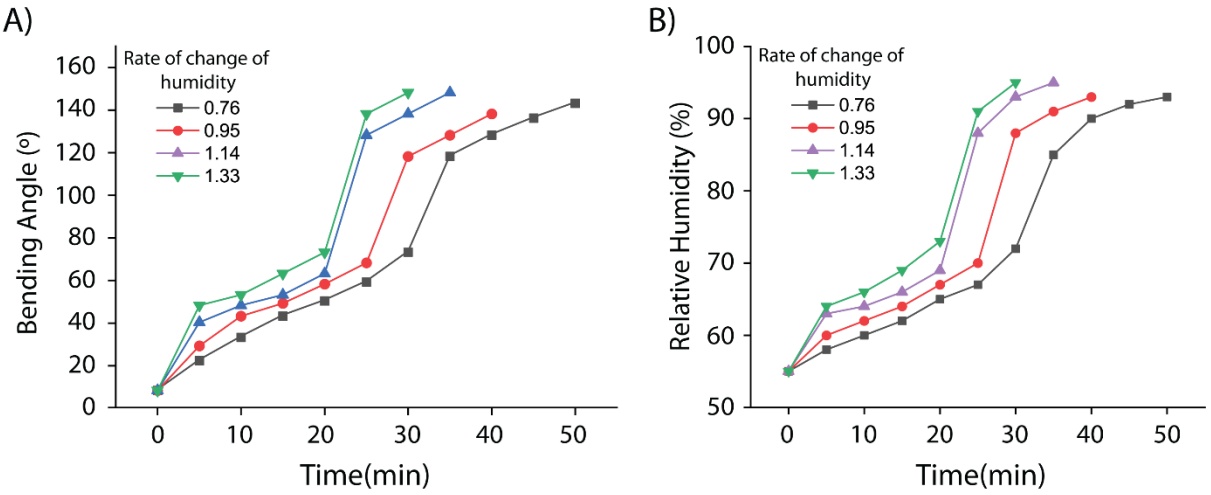

Figure S13. A) Bending angle exhibited by the BP@ODA actuator; B) Change in relative humidity as a function of time at different rates of change of humidity.

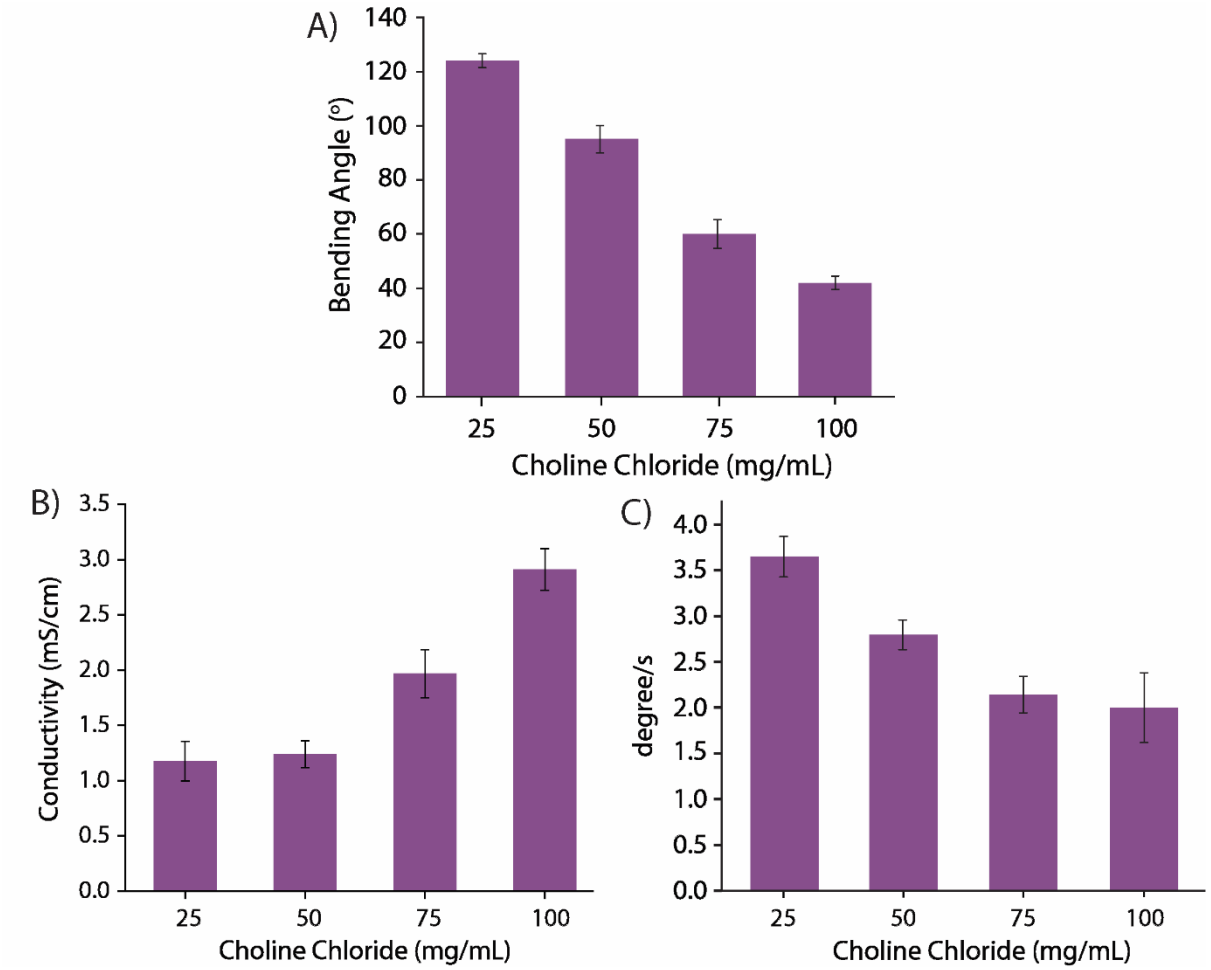

Figure S14. Performance of the actuator containing different concentrations of choline chloride: A) Bending angle; B) Conductivity; and C) Bending angle as a function of time, of the actuator at different concentrations of choline chloride, i.e., 25 mg/mL, 50 mg/mL, 75 mg/mL, and 100 mg/mL.

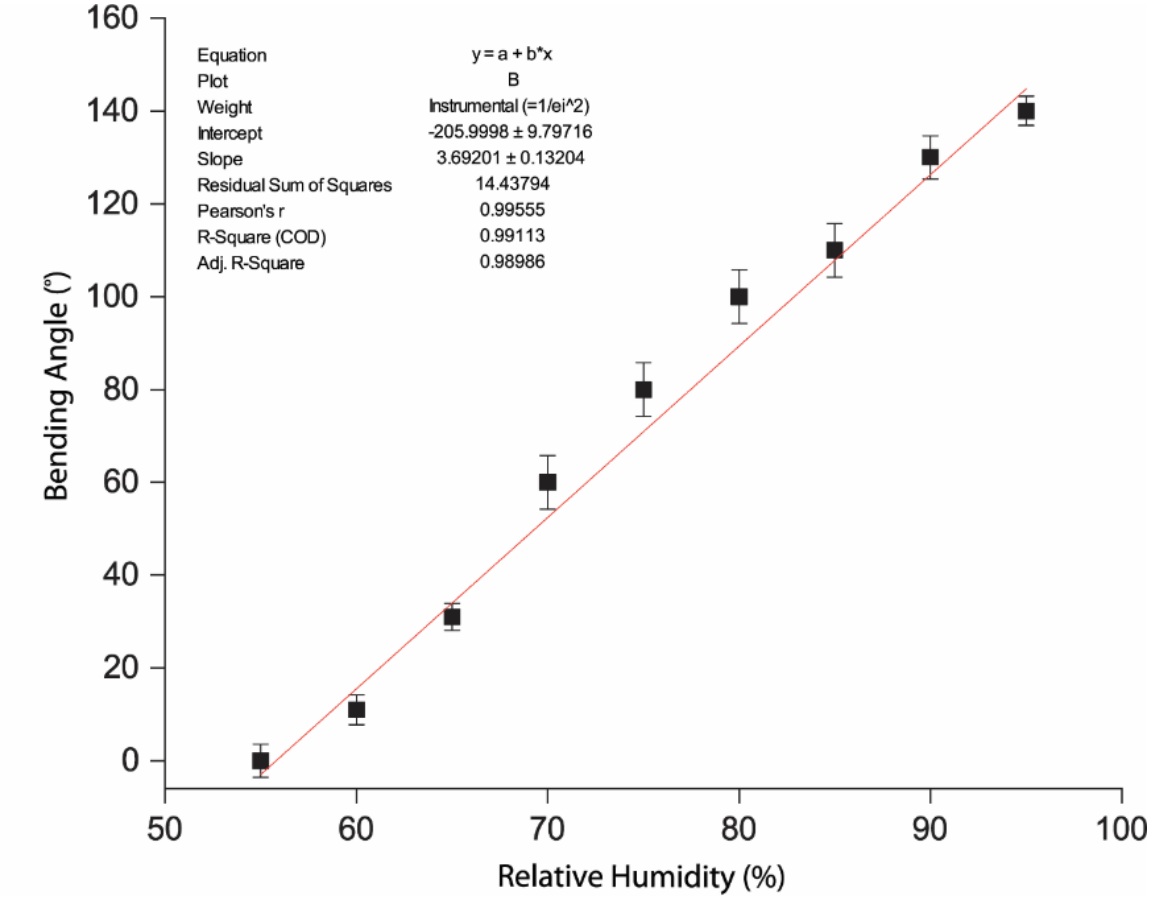

Figure S15. Linear bending angle calibration curve of the actuator with the change in the relative humidity.

Table S1. Comparative data of the thickness of the ODA coating and BP layer of the BP@ODA gels.

Sl. No.	ODA coating thickness (µm)	BP layer thickness (µm)	Thickness Ratio (ODA coating : BP layer)
1	33.26	332.9	0.09
2	33.56	333.4	0.10
3	35.94	341.9	0.10
4	34.94	341.4	0.10
5	34.40	348.0	0.09

Table S2. Comparative data for the current work and reported moisture-responsive actuators.

Material	Structure	Bending Angle (in degrees)	Actuation Rate	Actuation Mechanism	Reference
GO[1]	Monolayer	80° - 140°	30 °/s	Humidity Gradient	1
PDMS-CNT/Chitosan[2]	Bilayer	0° - 224°	3.75 °/s	Material Gradient	2
CLCP[3]	Monolayer	0° - 85°	-	Humidity Gradient	3
CNC-poly(PEGDMA)[4]	Monolayer	135°	4.6 °/s	Humidity Gradient	4
PVA/PAAm[5]	Monolayer	87°	1.68 °/s	Humidity Gradient	5
BP@ODA	Monolayer	140°	3.875 °/s	Uniform Exposure to Moisture	This work
BCNF/PDA[6]	Monolayer	133°	16.6 °/s	Humidity Gradient	6

References

[1] Y. Ge, R. Cao, S. Ye, Z. Chen, Z. Zhu, Y. Tu, D. Ge, X. Yang, *Chem. Commun.* **2018**, *54*, 3126-3129.

[2] H. Xu, X. Xu, J. Xu, S. Dai, X. Dong, F. Han, N. Yuan, J. Ding, *J. Mater. Chem. B* **2019**, *7*, 7558-7565.

[3] X. Zheng, S. Guan, C. Zhang, T. Qu, W. Wen, Y. Zhao, A. Chen, *Small* **2019**, *15*, 1900110.

[4] W. Ge, F. Zhang, D. Wang, Q. Wei, Q. Li, Z. Feng, S. Feng, X. Xue, G. Qing, Y. Liu, *Small* **2022**, *18*, 2107105.

[5] J. Guo, H. Zhang, T. Cui, J. Li, M.-H. Li, J. Hu, *Adv. Mater. Technol.* **2023**, *8*, 2300603.

[6] X. Xu, L. Yang, X. Xiong, Y. Zhang, J. Liu, Y. Hu, *ACS Appl. Polym. Mater.* **2025**, *7*, 10635-10644.